




# High endothelial venule is a surrogate biomarker for T-cell inflamed tumor microenvironment and prognosis in gastric cancer

Hyung Soon Park,<sup>1</sup> Yoo Min Kim,<sup>2</sup> Sewha Kim,<sup>3</sup> Won Suk Lee,<sup>4</sup> So Jung Kong,<sup>4</sup> Hannah Yang,<sup>4</sup> Beodeul Kang,<sup>4</sup> Jaekyung Cheon ,<sup>4</sup> Su-Jin Shin,<sup>5</sup> Chan Kim ,<sup>4</sup> Hong Jae Chon <sup>4</sup>

**To cite:** Park HS, Kim YM, Kim S, *et al.* High endothelial venule is a surrogate biomarker for T-cell inflamed tumor microenvironment and prognosis in gastric cancer. *Journal for ImmunoTherapy of Cancer* 2021;**9**:e003353. doi:10.1136/jitc-2021-003353

► Additional supplemental material is published online only. To view, please visit the journal online (<http://dx.doi.org/10.1136/jitc-2021-003353>).

HSP, YMK and SK contributed equally.

Accepted 27 September 2021



© Author(s) (or their employer(s)) 2021. Re-use permitted under CC BY-NC. No commercial re-use. See rights and permissions. Published by BMJ.

For numbered affiliations see end of article.

**Correspondence to**  
Dr Hong Jae Chon;  
minidoctor@cha.ac.kr

Dr Chan Kim; chan@cha.ac.kr

## ABSTRACT

**Background** High endothelial venule (HEV) is a specialized vasculature for lymphocyte trafficking. While HEVs are frequently observed within gastric cancer (GC), the vascular-immune interaction between HEV and tumor-infiltrating lymphocytes (TILs) has not been well elucidated. In this study, we aimed to unveil the potential value of HEVs as a surrogate marker for T-cell inflamed immune microenvironment in GC using a large number of prospectively collected surgical specimens of GC.

**Methods** We included 460 patients with GC who underwent surgical resection. Nanostring PanCancer immune profiling was performed to evaluate the immunological phenotype of GCs. HEV density and three distinct patterns of TILs (Crohn-like lymphoid reaction, peritumoral lymphoid reaction, and intratumoral lymphoid reaction) were analyzed for their relationship and evaluated as prognostic factors for relapse-free survival (RFS) and overall survival (OS).

**Results** HEV-high GC revealed increased infiltration by immune cell subsets, including dendritic cells, CD8<sup>+</sup> cytotoxic T cells, and CD4<sup>+</sup> helper T cells. In addition, HEV-high GC demonstrated increased immune-modulating chemokines, type I or II interferon pathway, and immune checkpoints, all of which indicate the inflamed tumor microenvironment (TME). All three distinct patterns of TILs were associated with HEV density. In survival analysis, patients with HEV-high GC displayed significantly longer RFS and OS than those with HEV-low GC ( $p < 0.001$  for RFS,  $p < 0.001$  for OS). Multivariate analysis demonstrated that HEV was the most significant immunological prognostic factor for RFS (patients with high HEV compared with those with low HEV; HR 0.412, 95% CI 0.241 to 0.705,  $p = 0.001$ ) and OS (HR 0.547, 95% CI 0.329 to 0.909,  $p = 0.02$ ) after adjustment for age, stage, and TIL.

**Conclusion** HEV is the most significant immunological prognosticator for RFS and OS in resected GC, indicating inflamed TME.

## BACKGROUND

Gastric cancer (GC) is a heterogeneous disease in terms of histological and molecular characteristics.<sup>1–4</sup> In the past 50 years, it has been histologically classified as

either intestinal or diffuse type according to Lauren's criteria.<sup>2,5</sup> With the advent of comprehensive molecular profiling using next-generation sequencing, several studies have tried to classify GC into distinct molecular subtypes.<sup>3,6,7</sup> Recently, with the introduction of immune checkpoint inhibitors (ICIs) for systemic treatment of advanced cancers, new attempts have been made to categorize tumors into immunological subtypes with distinct immune profiles.<sup>8–14</sup> Because tumor-infiltrating lymphocytes (TILs) play a decisive role in anticancer immunity and are closely related to prognosis and responses to cancer immunotherapy in various human malignancies, tumors can be classified as being either T-cell inflamed or non-inflamed, depending on TILs residing in the tumor microenvironment (TME).<sup>8,10,15–18</sup> The close interplay between TILs and tumor cells is critical for determining the magnitude of overall anticancer immune response.<sup>8,10</sup> However, most previous studies mainly focused on the absolute amounts of TILs, not on the patterns of lymphocyte infiltration within TME.

High endothelial venule (HEV) is a unique vasculature type physiologically found in secondary lymphoid organs, such as lymph nodes, and it enables lymphocytes to move in and out of the lymph nodes from systemic circulation.<sup>19–21</sup> Intriguingly, in addition to performing such physiological function in lymphoid organs, ectopic HEV can be formed and observed in pathological conditions, such as chronic inflammation or tumor.<sup>21–24</sup> Previously, high density of ectopic HEV within the tumor is known to be a favorable prognostic factor for survival in solid tumors, such as breast cancer, head and neck cancer, and malignant melanoma.<sup>24,25</sup> Tumor HEV has also been proposed to be an important

determinant in the process of intratumoral lymphocyte trafficking.<sup>10 21 24</sup> From the coexistence of HEV in the lymphocyte-rich tumor area, tumor HEV is suggested to cooperate with lymphocytes and aid their entry for transmigrating endothelial barriers.<sup>26 27</sup> Moreover, HEV has been reported to be associated with other subtypes of T cells, such as memory T and B cells within TME.<sup>27</sup> Furthermore, high densities of tumor HEV correlate with lymphotoxin-producing dendritic cells (DCs) and facilitate lymphocyte-mediated tumor cell death.<sup>24 25</sup>

In GC, the clinicopathological characteristics and prognostic role of HEV remain poorly investigated, and their relationship with TILs has not been elucidated well. Here, we comprehensively analyzed HEV and different histological patterns of TILs in GC, using whole surgical specimens obtained from a large, prospectively collected cohort of GC, and aimed to elucidate the potential value of HEV as a surrogate biomarker for anticancer immunity in GC.

## METHODS

### Patient and tissue specimen

This study included 460 patients who underwent curative surgical resection for GC at CHA Bundang Medical Center (Seongnam, Korea) and Yonsei University Health System (Seoul, Korea) between January 2009 and December 2010. Patients who had preoperative neoadjuvant chemotherapy or who had distant metastases at the time of diagnosis were excluded. Clinicopathological data, including patient's age at initial diagnosis, tumor location, histological subtype, Lauren type, pathological stage, tumor recurrence, and death, were extracted from a prospectively maintained database that had a predesigned data collection format. All H&E-stained slides for each case were reviewed by experienced pathologists (SK and SJS) to select the most representative tumor block with the highest invasion depth or largest tumor volume. The average number of slides required for selecting a representative slide was 8.1 (range 5–22). Histological subtypes were classified based on the *WHO Classification of Tumors of the Digestive System*, Fourth Edition. Pathological stage was determined according to the *American Joint Committee on Cancer (AJCC) Staging Manual*, Eighth edition.

### HEV immunohistochemistry

MECA-79, an L-selectin ligand, was selected as the specific marker of HEV in this study.<sup>22</sup> Immunohistochemistry for MECA-79 was performed on the surgically resected specimens of all patients included in the study. All immunohistochemistry was performed on whole tissue sections of the representative formalin-fixed paraffin-embedded (FFPE) blocks in order to overcome the limitation of the tissue microarray method. Briefly, 4 µm FFPE sections were transferred to adhesive slides and dried at 60°C for 30 min. They were then incubated with anti-peripheral node addressin (PNAd) (rat, clone MECA-79; Santa Cruz), anti-CD8 (rabbit, clone SP57; Ventana), anti-CD4 (rabbit,

clone SP35; Abcam), anti-FoxP3 (mouse, clone 236A/E7; Abcam), and anti-PD-L1 (rabbit, clone SP263; Ventana) at 4°C, overnight. Immune detection was achieved by the addition of secondary antibodies, followed by incubation with peroxidase-labeled streptavidin and 3,3'-diaminobenzidine as the chromogenic substrate. Slides were counterstained with Harris hematoxylin.

Tumor boundary was delineated by the pathologists, and the number of MECA-79-positive vessels within the tumor boundary was manually counted under the microscope. The tumor area was then measured using a computerized image analysis program (ImageJ, <http://rsb.info.nih.gov/ij/>). To overcome intratumoral heterogeneity in evaluating the HEV quantity, HEV density (number of HEVs/cm<sup>2</sup>), calculated as the number of HEVs divided by the tumor area, was used for analysis. Lymphocytes stained with anti-CD8, anti-CD4, and anti-Foxp3 and the tumor stained with anti PD-L1 were also quantified with the ImageJ program on tumor slides available for evaluating HEV density.

### RNA isolation and NanoString gene expression analysis

Total RNA was extracted from whole tumor lysates using TRIzol (Invitrogen) and purified with ethanol. RNA quality was confirmed with a fragment analyzer (Advanced Analytical Technologies, Iowa, USA). Immune profiling was performed with a digital multiplexed NanoString nCounter PanCancer Immune Profiling panel (NanoString Technologies), using 100 ng of total RNA isolated from tumor tissues. Data analysis was performed with nSolver software (NanoString Technologies). The mRNA profiling data was normalized by housekeeping genes and analyzed with R software ([www.r-project.org/](http://www.r-project.org/)), as previously described.<sup>28 29</sup>

### Histological assessment of TIL patterns

TIL patterns were independently evaluated in three categories: Crohn-like lymphoid reaction (CLR), peritumoral lymphoid reaction (PLR), and intratumoral lymphoid reaction (ILR). These TIL patterns were scored by interpreting the most representative slides of 460 tumors. First, CLR was defined as nodular lymphoid aggregate with or without a germinal center, observed either inside or along the tumor border. The number of CLRs was counted under low-power magnification (×40), and it was semiquantitatively scored as 0 (absent), 1 (occasional, 1–3 CLRs/low power field), 2 (moderate, 4–10 CLRs/low power field), or 3 (numerous CLRs).<sup>30 31</sup> Mucosa-associated lymphoid tissue (which is a lymphoid aggregate within the mucosa or just beneath the muscularis mucosa) was not counted as CLR. Second, PLR was defined as band-like lymphocytic infiltration along the invasive margin, and scored according to Klintrup criteria as follows: score 0, no infiltration; 1, mild and patchy infiltration; 2, prominent band-like infiltration; and 3, florid, cup-like infiltration.<sup>32</sup> Third, ILR was defined as lymphocytic infiltration into the stroma between cancer cells or lymphocytes in direct contact with cancer cells. Because

there is no consensus yet on TILs scoring in GC, this study followed the recommendations of the International TILs Working Group for breast cancer.<sup>33</sup> The stromal TILs were measured as the percentage of the total stroma area that was occupied by mononuclear inflammatory cells. It was scored as 0 (few lymphocytes), 1 (<10%), 2 (10–50%), and 3 (>50%).

### Statistical analysis

Data were analyzed using SPSS software for Windows V.20.0. Fisher's exact tests or  $\chi^2$  tests were used to compare categorical variables. Analysis of variance tests with Bonferroni post hoc analysis were used to compare continuous variables. Relapse-free survival (RFS) was calculated as the time from surgery to initial local or systemic recurrence. Overall survival (OS) was calculated as the time from surgery to death from any cause or to the last follow-up date. Survival analyses were performed using the Kaplan-Meier method with log-rank tests. Multivariate analysis was performed with Cox's regression. A *p* value of <0.05 was considered statistically significant.

## RESULTS

### HEV-high GC represents T-cell inflamed tumor

HEV density was thoroughly evaluated in whole surgically-resected tumor sections and categorized as being either low or high, based on the median value of HEV density (27.8/cm<sup>2</sup>). In HEV-high tumors, CD8<sup>+</sup> or CD4<sup>+</sup> lymphocytes preferentially accumulated near MECA79-positive HEVs (figure 1A,B). There was no significant difference in regulatory T cells (Tregs) between HEV-low and HEV-high tumors (online supplemental figure S1). We evaluated the immunogenic signature according to HEV status, using PanCancer Immune Profiling panel (NanoString Technologies). HEV-high tumors had differentially expressed gene profiles, including immune checkpoints, TME, and chemokines, compared with HEV-low tumors (figure 1C). Volcano plot showed the distinct immune signature suggestive of T-cell inflamed TME in HEV-high tumors, including activated DC, type I interferon (IFN) pathway, and immune-potentiating chemokines (figure 1D). Consistently, these immunological phenotypes were also identified in gene ontology enrichment analysis (figure 1E).

We specifically evaluated immune cell-type subsets according to HEV status (figure 2A,B). As expected, immune gene signatures of DCs (*XCRI*, *FLT3*, *CD1C*, *LAMP3*, and *CD209*), CD8 T cells (*CD8* and *GZMM*), CD4 T cells (*IL26*), and B cells (*CD19*) were significantly up-regulated in HEV-high tumors compared with HEV-low tumors. However, genes related to natural killer (NK) cells and Tregs were not different between HEV-high and HEV-low tumors. Chemokines related to recruitment of effector T cells (*CCL8*, *CCL2*, and *CCL3*) and interleukins (ILs) related to tertiary lymphoid structure (*IL-7* and *IL-23*) were upregulated in HEV-high tumors (figure 2C,D). However, there was no significant correlation between the gene expression of the T-cell subtype (*CD8* and *CD4*) and

recruiting chemokine ligands (*CCL8*, *CCL3*, and *CCL3*), except for *CD8* expression and *CCL8* (online supplemental figure S2). In addition to immune cell subsets, various TME genes were also analyzed (figure 2E). Genes related to T-cell exclusion phenotype were significantly downregulated in HEV-high tumors. Next, transcripts with type I or II IFN pathway, which are related to T-cell priming and T-cell recruitment, and other adaptive immunity were also induced in HEV-high tumors. Lastly, inhibitory immune checkpoint (*PDCD1* and *TIGIT*) and agonistic immune checkpoint (*ICOS*, *TNFRSF4*, and *TNFRSF9*) were induced in HEV-high tumors. Overall, HEV-high GCs had the characteristics of T-cell inflamed TME.

### HEV density is associated with distinct clinical characteristics in GC

For further clinicopathological analyses, 452 patients with GC who underwent curative gastrectomy were evaluated for HEV and TILs. The baseline characteristics of the patients are outlined in table 1. The majority of patients were men (65.7%), and the median age at initial diagnosis was 58 years (range 23–86 years). Histological subtype was well-differentiated (WD) or moderately differentiated (MD) adenocarcinoma in 172 (38.1%) patients and poorly differentiated (PD) adenocarcinoma or signet ring cell (SRC) carcinoma in 280 (61.9%) patients. Median follow-up duration was 36.8 months (range 0–56.6 months). Tumor recurrence, either local or systemic, occurred in 77 patients (17.0%), and 78 patients (17.3%) died.

Patients were classified into HEV-low (*n*=226) and HEV-high (*n*=226) tumor groups based on the median value of HEV density, and clinicopathological parameters were compared between the two groups (table 1). High HEV density was frequently observed in female patients (*p*=0.010), tumors with PD/SRC histology (*p*=0.026), Lauren diffuse-type tumors (*p*=0.019), tumors in the upper and middle third of the stomach (compared with lower third or whole stomach involvement, *p*=0.001), tumors with no serosal exposure (pT1–3) (compared with pT4, *p*<0.001), tumors with no nodal metastasis (pN0) (*p*=0.001), and tumors with lower TNM stage (I and II) (compared with stage III, *p*<0.001).

### Degree of TIL infiltration correlated with HEV density in GC

Since we found that HEV-high tumor was associated with increased T-cell subset in NanoString Immune Profiling analysis, we carefully analyzed the patterns and degrees of lymphocyte infiltrations in the surgical specimens of GC and identified three distinct subtypes: CLR, PLR, and ILR (figure 3A). Representative microscopic images for each subtype, with their various scores, are shown in figure 3B. Prominent lymphocyte infiltration, which was defined as a score of ≥2, was observed in 38%, 32%, and 26% of cases for CLR, PLR, and ILR, respectively (figure 3C). Most patients (98.7%) had a score of 1 or more in any of the three TIL patterns. A score of 1 or more in all three TIL



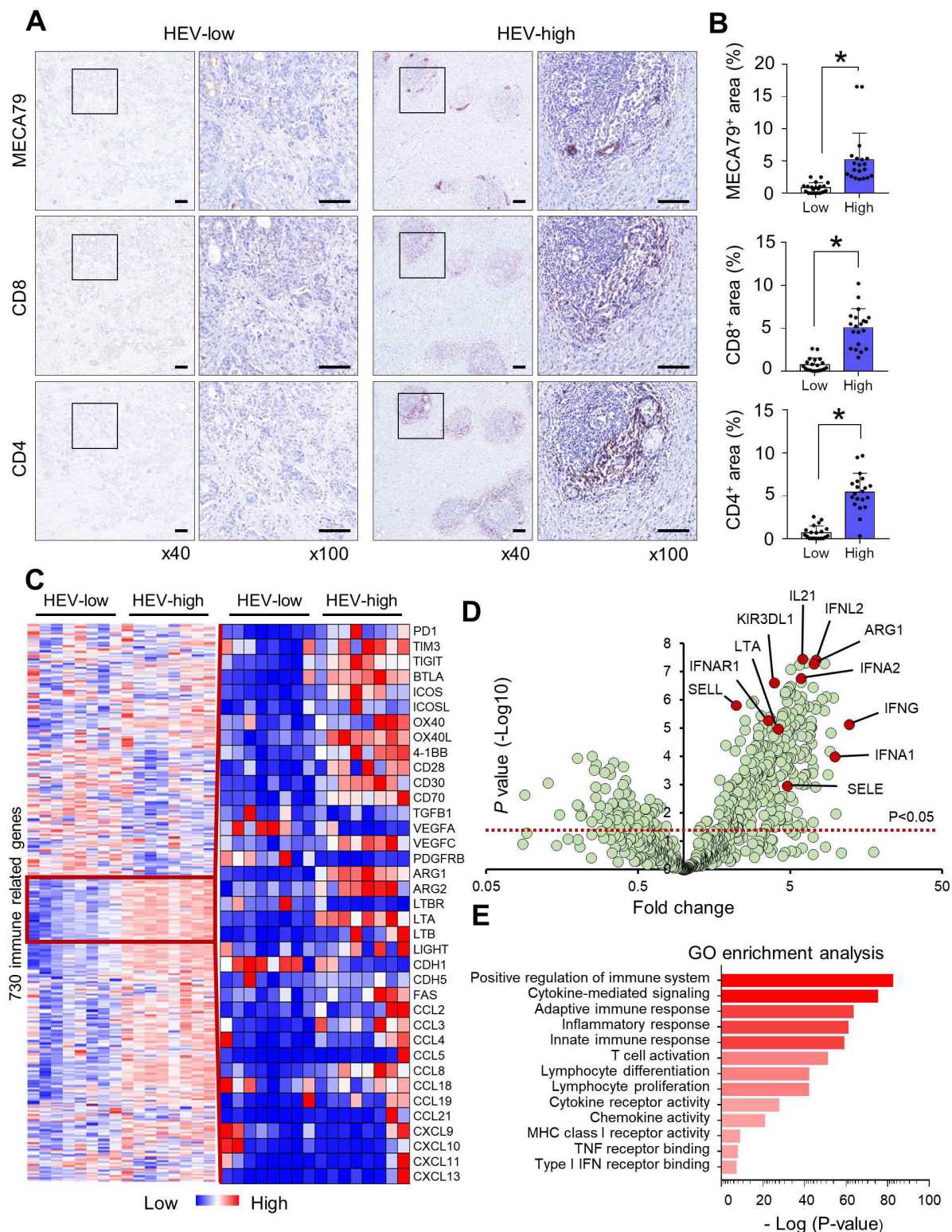


**Figure 1** HEV density was a surrogate marker for T-cell inflamed TME. (A) HEV expression (detected by MECA-79 staining) in surgically resected GC tissue was categorized into low and high status based on the median value of HEV density (27.8/cm<sup>2</sup>). Lymphocytes were stained with anti-CD8 and anti-CD4 antibodies for evaluating their relationship with HEV density. Scale bars: 200  $\mu$ m. (B) Quantification of the MECA-79 area and the CD8<sup>+</sup> and CD4<sup>+</sup> areas according to the HEV-low and HEV-high groups was performed, and their significant correlations are shown. Values are presented as mean $\pm$ SEM. (C) The differences in the expression of 730 immune-related genes were evaluated, and genes for immune checkpoints, TME, and chemokines varied with HEV density. (D) Volcano plot summarizing the effects of HEV density on immune-related gene expression. Red line,  $p < 0.05$ . (E) GO term enrichment analysis revealed 13 statistically significant biological processes controlled by differentially expressed genes among patients with high HEV density. \* $P < 0.05$ . GC, gastric cancer; GO, gene ontology; HEV, high endothelial venule; IFN, interferon; MHC, major histocompatibility complex; TME, tumor microenvironment; TNF, tumor necrosis factor.



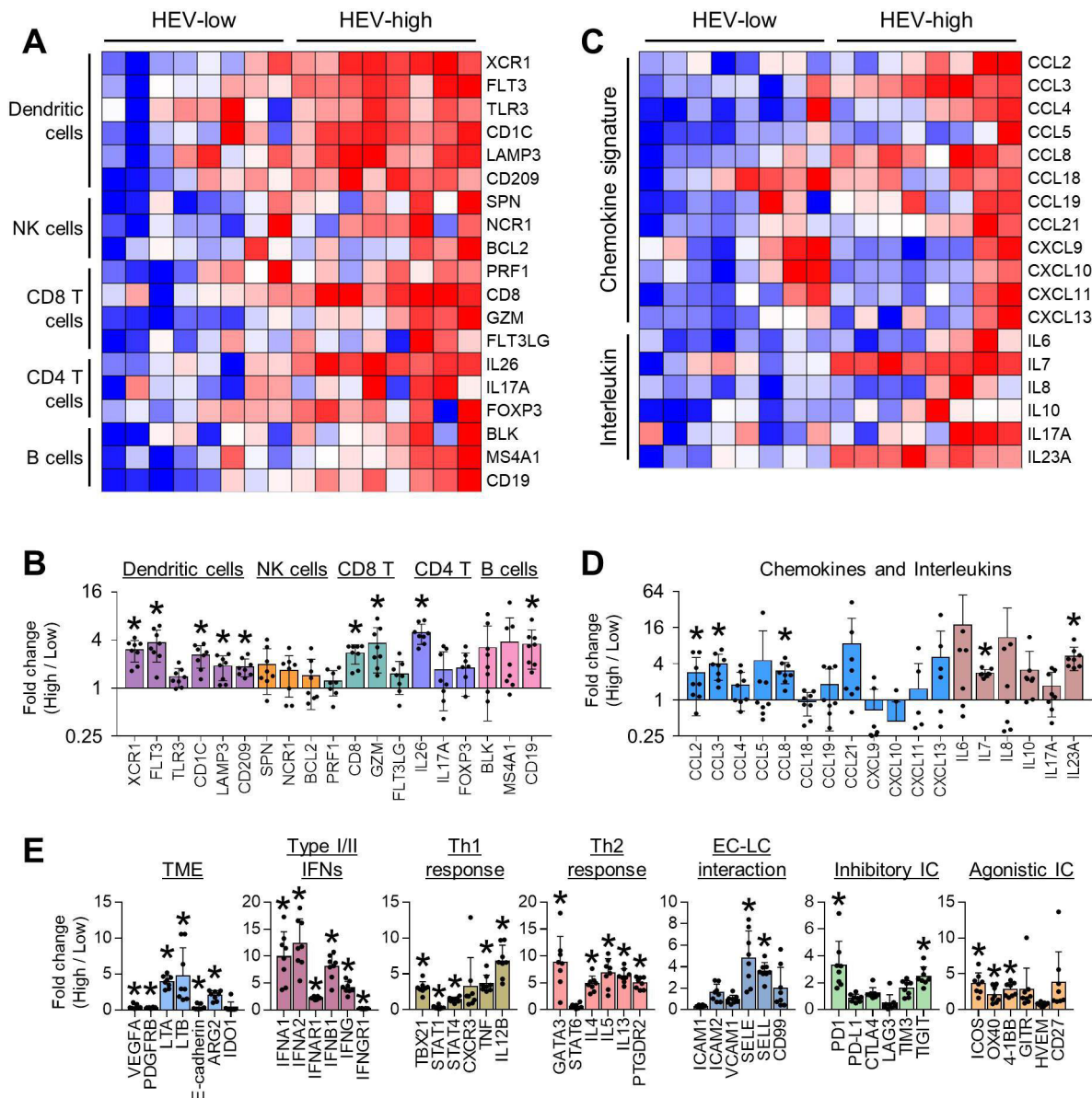


**Figure 2** Immune-related gene expression profile explained the anti-tumor immunity of HEV-high GC. (A) HEV-high GC had increased expression of immune cell subsets, including dendritic cells, cytotoxic and helper T cells, and B cells. (B) Fold changes of gene expression of immune cell subsets in HEV-high GC compared to HEV-low GC. Values are presented as mean $\pm$ SEM. \* $P$ <0.05. (C) Gene expression of immune-modulating chemokines and interleukins was higher in HEV-high GC. (D) Fold changes of chemokines and interleukins in HEV-high GC compared with HEV-low GC. Values are presented as mean $\pm$ SEM. \* $P$ <0.05. (E) Comparison of gene expression related to TME, type I or II interferon, Th1 and Th2 response, EC-LC interaction, and inhibitory and agonistic immune checkpoint between HEV-high and HEV-low GC. Values are presented as mean $\pm$ SEM. \* $P$ <0.05. EC, endothelial cell; GC, gastric cancer; HEV, high endothelial venule; IC, immune checkpoint; IFN, interferon; LC, lymphocyte; NK, natural killer; TME, tumor microenvironment.

patterns was seen in 307 (66.7%) patients, and a score of 0 in all three TIL patterns was seen in 6 (1.3%) patients.

Next, we analyzed the clinicopathological differences of the tumors, depending on the degree of each lymphoid reaction pattern (online supplemental table S1). The histological type and Lauren classification associated with CLR were different from those associated with PLR or ILR. Prominent CLR was more commonly observed in PD/SRC tumors and diffuse tumor type of Lauren classification, but prominent PLR and ILR were more common in WD/MD tumors and the intestinal type. Similar clinical

factors were associated with all three lymphoid reactions. Tumor location in the upper third of the stomach and TNM stage two or three were associated with score two or three for all three types of lymphoid reactions.

We also evaluated the correlation between HEV density and lymphoid reaction scores for the three patterns of TIL (figure 3D-F). We found significant positive correlations between HEV density and lymphoid reaction score in all three patterns; HEV density was lowest in tumors with poor lymphoid reaction (score 0), while it was highest in tumors with prominent lymphoid reaction (score two or

**Table 1** Comparison of the clinicopathological factors according to the HEV density

Parameter	N=452 (%)	Low HEV density	High HEV density	P value
		n=226 (%)	n=226 (%)	
Sex				0.010
Male	297 (65.7)	162 (71.7)	135 (59.7)	
Female	155 (34.3)	64 (28.3)	91 (40.3)	
Age (years)				0.452
<58	223 (49.3)	107 (47.3)	116 (51.3)	
≥58	229 (50.7)	119 (52.7)	110 (48.7)	
Histology				0.026
WD/MD	172 (38.1)	98 (43.4)	74 (32.7)	
PD/SRC	280 (61.9)	128 (56.6)	152 (67.3)	
Lauren type				0.019
Intestinal	220 (48.7)	123 (54.4)	97 (42.9)	
Diffuse	232 (51.3)	103 (45.6)	129 (57.1)	
Location				0.001
Upper	85 (18.8)	38 (16.8)	47 (20.8)	
Mid	105 (23.2)	39 (17.3)	66 (29.2)	
Low	258 (57.1)	145 (64.2)	113 (50.0)	
Whole	4 (0.9)	4 (1.8)	0 (0)	
T stage				<0.001
pT1	145 (32.1)	58 (25.7)	87 (38.5)	
pT2	59 (13.1)	27 (11.9)	32 (14.2)	
pT3	103 (22.8)	48 (21.2)	55 (24.3)	
pT4	145 (32.1)	93 (41.2)	52 (23.0)	
N stage				0.001
pN0	202 (44.7)	81 (35.8)	121 (53.5)	
pN1	71 (15.7)	42 (18.6)	29 (12.8)	
pN2	86 (19.0)	44 (19.5)	42 (18.6)	
pN3	93 (20.6)	59 (26.1)	34 (15.0)	
TNM stage				<0.001
I	139 (30.8)	57 (25.2)	82 (36.3)	
II	144 (31.9)	64 (28.3)	80 (35.4)	
III	169 (37.4)	105 (46.5)	64 (28.3)	
Crohn-like lymphoid reaction				<0.001
Score 0	75 (16.6)	59 (26.1)	16 (7.1)	
Score 1	203 (44.9)	112 (49.6)	91 (40.3)	
Score 2–3	174 (38.5)	55 (24.3)	119 (52.7)	
Peritumoral lymphoid reaction				0.163
Score 0	83 (18.4)	49 (21.7)	34 (15.0)	
Score 1	226 (50.0)	111 (49.1)	115 (50.9)	
Score 2–3	143 (31.6)	66 (29.2)	77 (34.1)	
Intratumoral lymphoid reaction				0.016
Score 0	29 (6.4)	21 (9.3)	8 (3.5)	
Score 1	304 (67.3)	154 (68.1)	150 (66.4)	
Score 2–3	119 (26.3)	51 (22.6)	68 (30.1)	
Overall lymphoid reaction				<0.001

Continued



Table 1 Continued

Parameter	N=452 (%)	Low HEV density	High HEV density	P value
		n=226 (%)	n=226 (%)	
Score 0–2	97 (21.5)	69 (30.5)	28 (12.4)	
Score 3–6	313 (69.2)	147 (65.0)	166 (73.5)	
Score 7–9	42 (9.3)	10 (4.4)	32 (14.2)	

HEV, high endothelial venule; MD, moderately differentiated; PD, poorly differentiated; SRC, signet ring cell; TNM, tumor, node, metastasis; WD, well differentiated.

3). Statistically, the lymphoid reaction pattern that had the most significant correlation with HEV density was CLR. The overall lymphoid reaction score was calculated by summation of the scores of the three lymphoid reaction patterns, which were then classified into low (score 0–2), middle (score 3–6), and high (score 7–9) lymphoid reaction groups. HEV density also significantly increased with increasing overall lymphoid reaction score ( $p<0.001$ ) (figure 3G).

#### HEV density has a stronger prognostic impact on RFS and OS than the conventional TILs pattern in GC

Survival outcomes, RFS and OS, were significantly affected by HEV status (figure 4A,B). Patients with HEV-high GC had significantly longer RFS than those with HEV-low GC (HR 0.281, 95% CI 0.167 to 0.473,  $p<0.001$ ). Moreover, HEV-high tumor was strongly associated with prolonged OS (HR 0.382, 95% CI 0.235 to 0.623,  $p<0.001$ ). Regarding histological pattern of TILs as a prognostic factor for RFS and OS, CLR and PLR were not significantly associated with survival outcome (figure 4C–F). However, patients with prominent ILR (score one or 2–3) had longer RFS than patients with low ILR (score 0) ( $p=0.028$ ) (figure 4G). Furthermore, prominent ILR was a significant prognostic factor for OS among patients with GC ( $p=0.019$ ) (figure 4H).

We compared the prognostic impact of HEV density and TIL patterns using multivariate analysis. HEV density was the most significant immunological prognosticator for RFS (patients with high HEV density compared with those with low HEV density: HR 0.412, 95% CI 0.241 to 0.705,  $p=0.001$ ) and OS (patients with high HEV density compared with low HEV density: HR 0.547, 95% CI 0.329 to 0.909,  $p=0.02$ ) (table 2). An ILR score of 2 or 3 was also an independent prognostic factor for RFS (HR 0.375, 95% CI 0.161 to 0.874,  $p=0.023$ ) and OS (HR 0.388, 95% CI 0.17 to 0.883,  $p=0.024$ ), compared with an ILR score of 0.

## DISCUSSION

In this study, we found that HEV density is a surrogate marker for T-cell inflamed tumor and a better prognostic factor for RFS and OS than TIL in patients with GC. We first comprehensively evaluated the immunological signature of HEV, using multiplexed immune profiling, and revealed that it is related to the distinct immune-related

gene expression profile. HEV-high GC had characteristics of T-cell inflamed TME, which are related to facilitated infiltration of T cells, robust activation of innate/adaptive immunity, and increased immune-modulating chemokines. These immune-related phenotypes correlated with enhanced adaptive immunity for tumor immunosurveillance and led to favorable prognosis in patients with HEV-high GC. We also evaluated and compared three distinct patterns of lymphoid reactions as prognostic factors using surgically resected tissue. Although ILR showed prognostic impact for both RFS and OS in the univariate analysis, its impact was reduced in multivariate analysis. However, HEV density demonstrated potent prognostic impact in both univariate and multivariate analyses, indicating that it is a better prognostic factor than ILR.

Currently, TILs are known as a good prognosticator in many studies, and the prognostic role of HEV was suggested by its association with infiltration by TILs such as cytotoxic T lymphocyte, central memory T lymphocytes, and B lymphocytes.<sup>8 24 27</sup> A previous study, through large-scale flow cytometric and quantitative reverse transcriptase PCR analyses, revealed that HEV-high tumor was associated with adaptive immunity and T-cell cytotoxicity.<sup>27</sup> Consistently, immune gene signature we revealed can provide clues regarding the underlying mechanism of antitumor T-cell immunity within HEV-high GC through more abundant gene expression patterns with DC activation signaling, type I or II IFN signaling, and enriched lymphoid chemokines. The IL level was known to have distinct patterns in GC, and we showed that IL-7 and IL-23 levels, which were known to contribute to the formation of the tertiary lymphoid structure, were increased in the HEV-high tumor.<sup>34–36</sup> NK cells and Tregs did not show differences according to HEV density. A previous study reported that Tregs suppressed HEV development, but differences in the number of Tregs between the HEV-low and HEV-high tumors were not observed.<sup>37 38</sup> To reveal the relatedness between HEV and other immune cell types, further studies are needed. We also identified that HEV-high GC has more upregulated multiple immune checkpoints, such as PD-1 and TIGIT, than HEV-low GC. Taken together, these results suggest that HEV is not merely a surrogate marker for TILs, but rather represents an immunocompetent TME in which the cancer immunity cycle is effectively working.

In an early study on breast cancer, the prognostic role of HEV density was reported to be significant and favorable

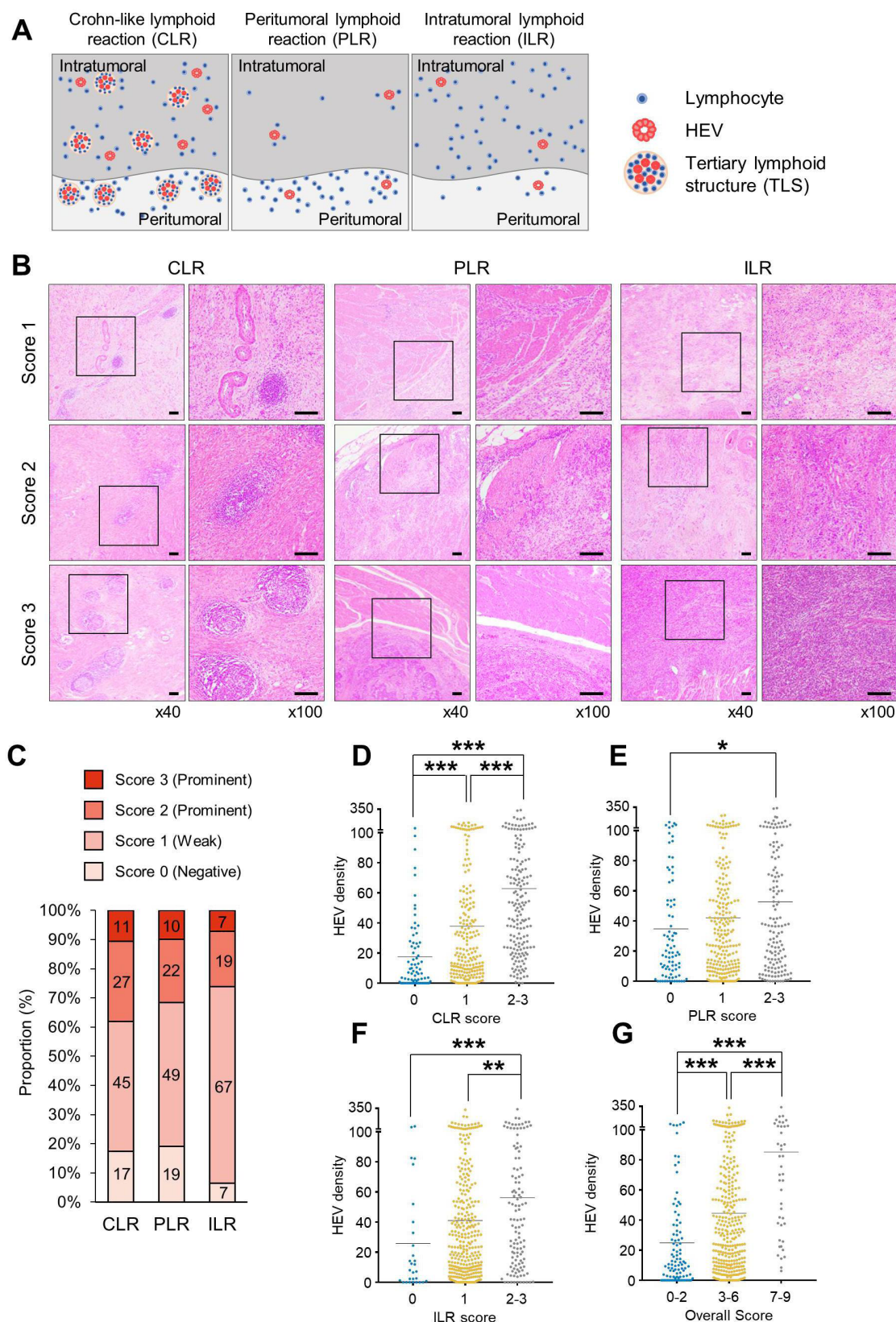


**Figure 3** All the distinct lymphoid reactions were significantly correlated with HEV density. (A) Three lymphoid reactions—CLR, PLR, and ILR—were evaluated with IHC stain. (B) Representative images of the three distinct lymphoid reactions, which were semiquantitatively scored as 1, 2, and 3. Scale bars: 200  $\mu$ m. (C) The distribution of 0–3 scoring of the three lymphoid reactions (CLR, PLR, and ILR) is shown. CLR (D), PLR (E), ILR (F), and overall lymphoid reaction scores (G) were positively correlated with HEV density. ANOVA with Bonferroni post hoc analysis was used (D–G). \* $P < 0.05$ , \*\* $P < 0.01$ , \*\*\* $P < 0.001$ . ANOVA, analysis of variance; CLR, Crohn-like lymphoid reaction; HEV, high endothelial venule; IHC, immunohistochemistry; ILR, intratumoral lymphoid reaction; PLR, peritumoral lymphoid reaction.



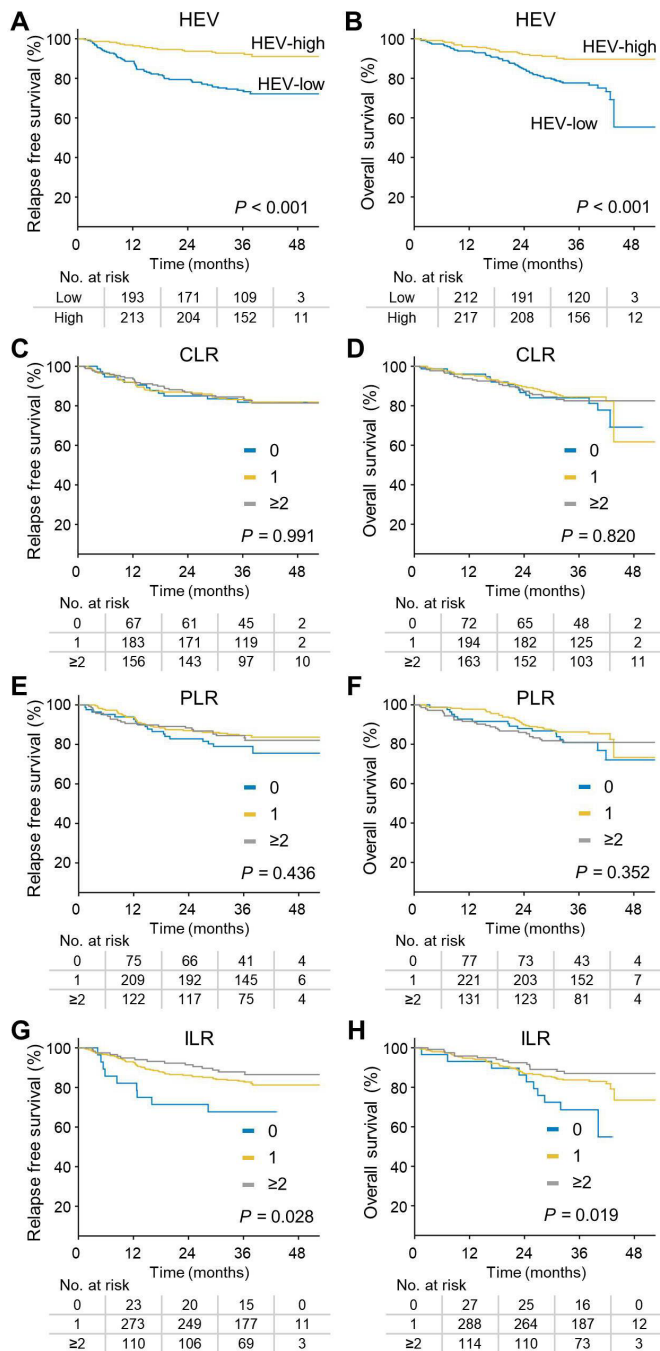


**Figure 4** HEV density and ILR score were significant prognostic factors for both RFS and OS. (A,B) Kaplan-Meier survival curve according to HEV density showed significant association with RFS (A) and OS (B) (log-rank test  $p < 0.001$  and  $p < 0.001$ , respectively). (C,D) Scoring of CLR was not significantly associated with RFS (C) and OS (D) (log-rank test  $p = 0.991$  and  $p = 0.82$ , respectively). (E,F) Scoring of PLR was not significantly associated with RFS (E) and OS (F) (log-rank test  $p = 0.436$  and  $p = 0.352$ , respectively). (G,H) Scoring of ILR was significantly associated with both RFS (G) and OS (H) (log-rank test  $p = 0.028$  and  $p = 0.019$ , respectively). CLR, Crohn-like lymphoid reaction; HEV, high endothelial venules; ILR, intratumoral lymphoid reaction; OS, overall survival; PLR, peritumoral lymphoid reaction; RFS, relapse-free survival.

for survival outcome.<sup>27</sup> Additionally, patients with HEV had increased PFS and OS with pharyngeal, laryngeal, or oral cancer.<sup>39,40</sup> Furthermore, patients with cutaneous melanoma showed a positive correlation between tumor regression and HEV density.<sup>41</sup> However, a previous study to elucidate the role of HEV using tissue microarray in GC did not demonstrate the prognostic role of HEV.<sup>23</sup> In our study, we demonstrated the prognostic role of HEV in GC by comprehensively analyzing whole tumor tissue retrieved from gastrectomy. Recently, several preclinical studies have demonstrated that the therapeutic efficacy of ICIs is significantly enhanced when the intratumoral HEV are expanded through therapeutic remodeling of the TME.<sup>42,43</sup> Although the predictive role of HEV in ICI has been less investigated, the tertiary lymphoid structure, which is an ectopic lymphoid structure with abundant HEV, was found to be a favorable biomarker for ICI therapy.<sup>44</sup> However, HEV was not always associated with the organized lymphoid structure and was often present within the loosely assembled lymphoid aggregates.<sup>45</sup> Moreover, HEV was a significant prognostic factor for RFS and OS in our study (data not shown), regardless of CLR, which resembles the tertiary lymphoid structure. Therefore, further clinical and translational studies are needed to evaluate HEV as a predictive biomarker for immunotherapy in metastatic GC.

TILs have been extensively studied in relation to the immunological milieu within various solid malignancies.<sup>8</sup> Many studies have quantitatively analyzed TILs and consistently reported their favorable prognostic impact in GC.<sup>18,46</sup> However, none of these studies qualitatively and comprehensively evaluated various histopathological patterns of TILs in GC, which have already been well described in colorectal cancer. Therefore, we analyzed the histopathological patterns of TILs and correlated those with HEV density in GC. Then, we compared the three distinct TIL patterns as a prognostic factor in these patients.

First of all, HEV density positively correlated with all three patterns of lymphoid reaction in GC, and CLR was the most significant lymphoid reaction pattern. Previously, prominent CLR has been identified as a significant prognosticator of favorable outcomes in colorectal cancer studies.<sup>31,32</sup> In our study, the CLR score in GC highly correlated with PD/SRC histology and diffuse type GC, and CLR was frequently observed in advanced GC. However, CLR score alone was not associated with survival outcome in GC. In a previous study, a subtype of lymphoepithelioma-like carcinoma (LELC) with CLR had better prognosis than conventional adenocarcinoma in Epstein-Barr virus-positive GC.<sup>47</sup> However, the significance of favorable prognosis of subtype with CLR in GC was less evident than those of LELC subtype, and it may suggest that intratumoral/peritumoral TILs are more important than CLR for host inflammatory response in GC. PLR score was also not associated with survival in our study. In other solid tumors, the prognostic role of peritumoral TILs has been less investigated than that of intratumoral TILs, and the impact of PLR on survival was not consistent in the previous studies.<sup>48,49</sup> Hennequin *et al.* reported that CD20<sup>+</sup> peritumoral lymphoid structure was associated with better RFS in GC,<sup>50</sup>

**Table 2** Univariate and multivariate analyses of recurrence-free and overall survival

Parameter	Recurrence-free survival				Overall survival			
	Univariate		Multivariate		Univariate		Multivariate	
	HR (95% CI)	P value	HR (95% CI)	P value	HR (95% CI)	P	HR (95% CI)	P value
Sex								
Male	1	0.261			1	0.393		
Female	0.753 (0.459 to 1.235)				0.809 (0.497 to 1.316)			
Age (years)								
<58	1	0.001	1	0.001	1	<0.001	1	<0.001
≥58	2.298 (1.425 to 3.704)		2.297 (1.421 to 3.712)		4.243 (2.448 to 7.354)		4.243 (2.444 to 7.367)	
Histology								
WD/MID	1	0.665			1	0.614		
PD/SRC	0.904 (0.573 to 1.427)				0.890 (0.567 to 1.398)			
Lauren type								
Intestinal	1	0.994			1	0.612		
Diffuse	0.998 (0.638 to 1.561)				0.891 (0.572 to 1.390)			
T stage								
pT1-2	1	<0.001	1	0.002	1	<0.001	1	0.003
pT3-4	4.870 (2.679 to 8.851)		2.637 (1.410 to 4.931)		3.465 (2.020 to 5.942)		2.383 (1.342 to 4.232)	
N stage								
pN0	1	<0.001	1	<0.001	1	<0.001	1	0.005
pN1-3	7.197 (3.587 to 14.440)		4.644 (2.236 to 9.646)		3.590 (2.069 to 6.232)		2.318 (1.282 to 4.190)	
Crohn-like lymphoid reaction								
Score 0	1	0.991			1	0.820		
Score 1	0.958 (0.505 to 1.816)				0.823 (0.447 to 1.515)			
Score 2-3	0.976 (0.508 to 1.873)				0.863 (0.464 to 1.604)			
Peritumoral lymphoid reaction								
Score 0	1	0.439			1	0.356		
Score 1	0.692 (0.393 to 1.218)				0.698 (0.390 to 1.250)			
Score 2-3	0.758 (0.409 to 1.404)				0.947 (0.516 to 1.737)			
Intratumoral lymphoid reaction								
Score 0	1	0.034	1	0.075	1	0.024	1	0.078
Score 1	0.477 (0.235 to 0.968)		0.554 (0.270 to 1.134)		0.468 (0.238 to 0.921)		0.586 (0.294 to 1.168)	
Score 2-3	0.336 (0.147 to 0.768)		0.375 (0.161 to 0.874)		0.332 (0.149 to 0.740)		0.388 (0.170 to 0.883)	
Overall lymphoid reaction								
Score 0-2	1	0.588			1	0.675		
Score 3-6	0.784 (0.467 to 1.315)				0.792 (0.472 to 1.330)			
Score 7-9	0.691 (0.278 to 1.722)				0.814 (0.344 to 1.927)			
HEV density								
Low	1	<0.001	1	0.001	1	<0.001	1	0.020
High	0.281 (0.167 to 0.473)		0.412 (0.241 to 0.705)		0.382 (0.235 to 0.623)		0.547 (0.329 to 0.909)	

.HEV, high endothelial venule; MD, moderate differentiated; OS, overall survival; PD, poorly differentiated; SRC, signet ring cell; WD, well differentiated.



but our study did not prove PLR as a significant prognostic factor. Thus, further studies are needed to identify the prognostic role of PLR in GC. Of the three lymphoid reactions, ILR was the only TILs-related prognostic factor of GC—the higher the ILR score, the more favorable the survival trend. In fact, the favorable prognostic role of intratumoral TILs has been frequently reported in GC studies with TILs.<sup>46</sup> Mainly, the relationship between CD8<sup>+</sup> TILs and better survival outcome has been reported, and intratumoral CD4<sup>+</sup> lymphocyte has also been reported as a good prognostic factor for GC.<sup>46</sup>

A strength of this study is that we evaluated the role of HEV as a prognostic factor in a large number of patients with GC. Second, we used whole surgical tumor sections, which fully reflected the overall TME, to evaluate the HEV density and pattern of TILs, instead of using tissue microarray. To precisely analyze intratumoral HEV, we did not simply check the presence of HEV expression. Rather, we analyzed HEV by quantifying the density of intratumoral HEV according to the tumor area, thereby more accurately reflecting the HEV expression level in the tumor. Furthermore, we thoroughly compared the association between HEV density and three different patterns of lymphoid reactions in GC, and we found that HEV correlated with all lymphoid reactions and was the most significant prognostic factor for RFS and OS, rather than TILs. Finally, comprehensive immune-related gene profiling was performed with high throughput, multi-gene technology according to HEV density, and it revealed that HEV was associated with T-cell inflamed tumor. The limitation of our study is that we did not classify subsets of TILs when evaluating the distinct patterns of TILs. Second, neoadjuvant chemotherapy was known to affect the immune cell recruitment and distribution. However, our study did not include patients with neoadjuvant chemotherapy, and the impact of chemotherapy on immune cells and the TME was not evaluated.

In conclusion, we demonstrated that HEV density is a surrogate marker for T-cell inflamed TME and is the most significant immunological prognostic factor for RFS and OS in patients with GC after surgical resection. Among the histopathological TIL patterns, only ILR showed favorable prognostic impact. Further studies are needed to investigate the relationship between HEV and therapeutic response to ICI therapy in GC.

#### Author affiliations

<sup>1</sup>Division of Medical Oncology, Department of Internal Medicine, St. Vincent's Hospital, College of Medicine, The Catholic University of Korea, Seoul, Korea (the Republic of)

<sup>2</sup>Department of Surgery, Yonsei University College of Medicine, Seoul, Korea (the Republic of)

<sup>3</sup>Department of Pathology, CHA Bundang Medical Center, CHA University School of Medicine, Seongnam, Gyeonggi-do, Korea (the Republic of)

<sup>4</sup>Medical Oncology, CHA Bundang Medical Center, CHA University School of Medicine, Seongnam, Gyeonggi-do, Korea (the Republic of)

<sup>5</sup>Department of Pathology, Gangnam Severance Hospital, Yonsei University College of Medicine, Seoul, Korea (the Republic of)

**Contributors** HSP, SK, CK, and HJC were responsible for the study concept and design. SK, WSL, SJK, CK, and HJC conducted the experiments. HSP, YMK, SK, HY, BK, JC, SJS, CK, and HJC performed data analysis. HSP, SK, CK, and HJC generated the figures and wrote and reviewed the manuscript. CK and HJC supervised the study, obtained funding, and drafted the manuscript. All authors read and approved the final manuscript.

**Funding** This work was supported by the National Research Foundation of Korea (NRF) grant funded by the Korea government (Ministry of Science and ICT (MSIT)) (NRF-2020R1A2C2004530 to CK, NRF-2020R1C1C1010722 to HJC). This work was also supported by the Korea Medical Device Development Fund grant funded by the Korea government (the MSIT, the Ministry of Trade, Industry and Energy, the Ministry of Health & Welfare, and the Ministry of Food and Drug Safety) (project number: KMDF202012D21-01 to CK).

**Competing interests** No, there are no competing interests.

**Patient consent for publication** Not applicable.

**Ethics approval** This study was approved by the institutional review boards of CHA Bundang Medical Center (IRB number 2017-11-0542) and Yonsei University Health System (IRB number 2019-2037).

**Provenance and peer review** Not commissioned; externally peer reviewed.

**Data availability statement** Data are available upon reasonable request.

**Supplemental material** This content has been supplied by the author(s). It has not been vetted by BMJ Publishing Group Limited (BMJ) and may not have been peer-reviewed. Any opinions or recommendations discussed are solely those of the author(s) and are not endorsed by BMJ. BMJ disclaims all liability and responsibility arising from any reliance placed on the content. Where the content includes any translated material, BMJ does not warrant the accuracy and reliability of the translations (including but not limited to local regulations, clinical guidelines, terminology, drug names and drug dosages), and is not responsible for any error and/or omissions arising from translation and adaptation or otherwise.

**Open access** This is an open access article distributed in accordance with the Creative Commons Attribution Non Commercial (CC BY-NC 4.0) license, which permits others to distribute, remix, adapt, build upon this work non-commercially, and license their derivative works on different terms, provided the original work is properly cited, appropriate credit is given, any changes made indicated, and the use is non-commercial. See <http://creativecommons.org/licenses/by-nc/4.0/>.

#### ORCID iDs

Jaekyung Cheon <http://orcid.org/0000-0001-8439-1739>

Chan Kim <http://orcid.org/0000-0001-9780-6155>

Hong Jae Chon <http://orcid.org/0000-0002-6979-5812>

#### REFERENCES

- Shah MA, Khanin R, Tang L, *et al.* Molecular classification of gastric cancer: a new paradigm. *Clin Cancer Res* 2011;17:2693–701.
- Chon HJ, Hyung WJ, Kim C. Differential prognostic implications of gastric signet ring cell carcinoma: stage adjusted analysis from a single high-volume center in Asia. *Ann Surg* 2017;265:946–53.
- Cancer Genome Atlas Research Network. Comprehensive molecular characterization of gastric adenocarcinoma. *Nature* 2014;513:202–9.
- Gullo I, Carneiro F, Oliveira C, *et al.* Heterogeneity in gastric cancer: from pure morphology to molecular classifications. *Pathobiology* 2018;85:50–63.
- Lauren P. The two histological main types of gastric carcinoma: diffuse and so-called intestinal-type carcinoma. *Apmis* 1965;64:31–49.
- Wang K, Yuen ST, Xu J, *et al.* Whole-genome sequencing and comprehensive molecular profiling identify new driver mutations in gastric cancer. *Nat Genet* 2014;46:573–82.
- Park HS, Kwon WS, Park S, *et al.* Comprehensive immune profiling and immune-monitoring using body fluid of patients with metastatic gastric cancer. *J Immunother Cancer* 2019;7:268.
- Gajewski TF, Schreiber H, Fu Y-X. Innate and adaptive immune cells in the tumor microenvironment. *Nat Immunol* 2013;14:1014–22.
- Zeng D, Li M, Zhou R, *et al.* Tumor microenvironment characterization in gastric cancer identifies prognostic and immunotherapeutically relevant gene signatures. *Cancer Immunol Res* 2019;7:737–50.
- Lee WS, Yang H, Chon HJ, *et al.* Combination of anti-angiogenic therapy and immune checkpoint blockade normalizes vascular-

- immune crosstalk to potentiate cancer immunity. *Exp Mol Med* 2020;52:1475–85.
- 11 Fuchs CS, Doi T, Jang RW, *et al.* Safety and efficacy of pembrolizumab monotherapy in patients with previously treated advanced gastric and gastroesophageal junction cancer. *JAMA Oncol* 2018;4:e180013.
  - 12 Kim CG, Kim C, Yoon SE, *et al.* Hyperprogressive disease during PD-1 blockade in patients with advanced hepatocellular carcinoma. *J Hepatol* 2021;74:350–9.
  - 13 Goh YH, Yoo J, Noh JH. Emerging targeted therapies in advanced bladder cancer. *Trans Cancer Res* 2017;6:S666–76.
  - 14 HJ A, Chon HJ, Kim C. Peripheral blood-based biomarkers for immune checkpoint inhibitors. *Int J Molecul Sci* 2021;22:9414.
  - 15 Ropponen KM, Eskelinen MJ, Lipponen PK, *et al.* Prognostic value of tumour-infiltrating lymphocytes (TILs) in colorectal cancer. *J Pathol* 1997;182:318–24.
  - 16 Adams S, Gray RJ, Demaria S, *et al.* Prognostic value of tumor-infiltrating lymphocytes in triple-negative breast cancers from two phase III randomized adjuvant breast cancer trials: ECoG 2197 and ECoG 1199. *J Clin Oncol* 2014;32:2959–66.
  - 17 Hegde PS, Karanikas V, Evers S. The where, the when, and the how of immune monitoring for cancer immunotherapies in the era of checkpoint inhibition. *Clin Cancer Res* 2016;22:1865–74.
  - 18 Lee HE, Chae SW, Lee YJ, *et al.* Prognostic implications of type and density of tumour-infiltrating lymphocytes in gastric cancer. *Br J Cancer* 2008;99:1704–11.
  - 19 Sautès-Fridman C, Lawand M, Giraldo NA, *et al.* Tertiary lymphoid structures in cancers: prognostic value, regulation, and manipulation for therapeutic intervention. *Front Immunol* 2016;7:407.
  - 20 Yang H, Lee WS, Kong SJ, *et al.* STING activation reprograms tumor vasculatures and synergizes with VEGFR2 blockade. *J Clin Invest* 2019;129:4350–64.
  - 21 Dieu-Nosjean M-C, Giraldo NA, Kaplon H, *et al.* Tertiary lymphoid structures, drivers of the anti-tumor responses in human cancers. *Immunol Rev* 2016;271:260–75.
  - 22 Girard J-P, Springer TA. High endothelial venules (HEVs): specialized endothelium for lymphocyte migration. *Immunol Today* 1995;16:449–57.
  - 23 Hong SA, Hwang HW, Kim MK, *et al.* High endothelial venule with concomitant high CD8+ tumor-infiltrating lymphocytes is associated with a favorable prognosis in resected gastric cancer. *J Clin Med* 2020;9:2628.
  - 24 Blanchard L, Girard J-P. High endothelial venules (HEVs) in immunity, inflammation and cancer. *Angiogenesis* 2021;12.
  - 25 Martinet L, Filleron T, Le Guellec S, *et al.* High endothelial venule blood vessels for tumor-infiltrating lymphocytes are associated with lymphotoxin  $\beta$ -Producing dendritic cells in human breast cancer. *J Immunol* 2013;191:2001–8.
  - 26 Ager A, May MJ. Understanding high endothelial venules: lessons for cancer immunology. *Oncoimmunology* 2015;4:e1008791.
  - 27 Martinet L, Garrido I, Filleron T, *et al.* Human solid tumors contain high endothelial venules: association with T- and B-lymphocyte infiltration and favorable prognosis in breast cancer. *Cancer Res* 2011;71:5678–87.
  - 28 Lee YS, Lee WS, Kim CW, *et al.* Oncolytic vaccinia virus reinvigorates peritoneal immunity and cooperates with immune checkpoint inhibitor to suppress peritoneal carcinomatosis in colon cancer. *J Immunother Cancer* 2020;8:e000857.
  - 29 Lee SJ, Yang H, Kim WR, *et al.* STING activation normalizes the intraperitoneal vascular-immune microenvironment and suppresses peritoneal carcinomatosis of colon cancer. *J Immunother Cancer* 2021;9:e002195.
  - 30 Graham DM, Appelman HD. Crohn's-like lymphoid reaction and colorectal carcinoma: a potential histologic prognosticator. *Mod Pathol* 1990;3:332–5.
  - 31 Ogino S, Nosho K, Irahara N, *et al.* Lymphocytic reaction to colorectal cancer is associated with longer survival, independent of lymph node count, microsatellite instability, and CpG island methylator phenotype. *Clin Cancer Res* 2009;15:6412–20.
  - 32 Klintrup K, Mäkinen JM, Kaupilla S, *et al.* Inflammation and prognosis in colorectal cancer. *Eur J Cancer* 2005;41:2645–54.
  - 33 Salgado R, Denkert C, Demaria S, *et al.* The evaluation of tumor-infiltrating lymphocytes (TILs) in breast cancer: recommendations by an International TILs Working Group 2014. *Ann Oncol* 2015;26:259–71.
  - 34 Madej-Michniewicz A, Budkowska M, Sałata D, *et al.* Evaluation of selected interleukins in patients with different gastric neoplasms: a preliminary report. *Sci Rep* 2015;5:14382.
  - 35 Błogowski W, Madej-Michniewicz A, Marczuk N, *et al.* Interleukins 17 and 23 in patients with gastric neoplasms. *Sci Rep* 2016;6:37451.
  - 36 Jing F, Choi EY. Potential of cells and cytokines/chemokines to regulate tertiary lymphoid structures in human diseases. *Immune Netw* 2016;16:271–80.
  - 37 Colbeck EJ, Jones E, Hindley JP, *et al.* Treg depletion licenses T Cell-Driven HEV neogenesis and promotes tumor destruction. *Cancer Immunol Res* 2017;5:1005–15.
  - 38 Martinet L, Le Guellec S, Filleron T. High endothelial venules (HEVs) in human melanoma lesions: major gateways for tumor-infiltrating lymphocytes. *Oncoimmunology* 2012;1:829–39.
  - 39 Karpathiou G, Dumollard JM, Gavid M, *et al.* High endothelial venules are present in pharyngeal and laryngeal carcinomas and they are associated with better prognosis. *Pathol Res Pract* 2021;220:153392.
  - 40 Wirsing AM, Rikardsen OG, Steigen SE, *et al.* Presence of tumour high-endothelial venules is an independent positive prognostic factor and stratifies patients with advanced-stage oral squamous cell carcinoma. *Tumor Biol.* 2016;37:2449–59.
  - 41 Avram G, Sánchez-Sendra B, Martín JM, *et al.* The density and type of MECA-79-positive high endothelial venules correlate with lymphocytic infiltration and tumour regression in primary cutaneous melanoma. *Histopathology* 2013;63:852–61.
  - 42 Allen E, Jabouille A, Rivera LB, *et al.* Combined antiangiogenic and anti-PD-L1 therapy stimulates tumor immunity through HEV formation. *Sci Transl Med* 2017;9:eaak9679.
  - 43 Peske JD, Thompson ED, Genta L, *et al.* Effector lymphocyte-induced lymph node-like vasculature enables naive T-cell entry into tumours and enhanced anti-tumour immunity. *Nat Commun* 2015;6:7114.
  - 44 Jacquemet N, Tellier J, Nutt SI, *et al.* Tertiary lymphoid structures and B lymphocytes in cancer prognosis and response to immunotherapies. *Oncoimmunology* 2021;10:1900508.
  - 45 Bento DC, Jones E, Junaid S, *et al.* High endothelial venules are rare in colorectal cancers but accumulate in extra-tumoral areas with disease progression. *Oncoimmunology* 2015;4:e974374.
  - 46 Lee JS, Won HS, Sun S. Prognostic role of tumor-infiltrating lymphocytes in gastric cancer: a systematic review and meta-analysis. *Medicine* 2018;97:e11769.
  - 47 Song H-J, Srivastava A, Lee J, *et al.* Host inflammatory response predicts survival of patients with Epstein-Barr virus-associated gastric carcinoma. *Gastroenterology* 2010;139:84–92.
  - 48 Sorbye SW, Kilvaer TK, Valkov A, *et al.* Prognostic impact of peritumoral lymphocyte infiltration in soft tissue sarcomas. *BMC Clin Pathol* 2012;12:5.
  - 49 Sabbatino F, Scognamiglio G, Liguori L, *et al.* Peritumoral immune infiltrate as a prognostic biomarker in thin melanoma. *Front Immunol* 2020;11:561390.
  - 50 Hennequin A, Derangère V, Boidot R, *et al.* Tumor infiltration by Tbet+ effector T cells and CD20+ B cells is associated with survival in gastric cancer patients. *Oncoimmunology* 2016;5:e1054598.